

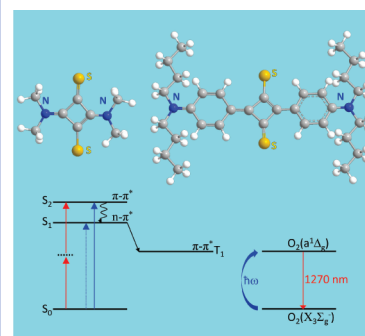
Near-Unity Quantum Yields for Intersystem Crossing and Singlet Oxygen Generation in Polymethine-like Molecules: Design and Experimental Realization

Scott Webster,^{*,†} Davorin Peceli,[†] Honghua Hu,[†] Lazaro A. Padilha,[†] Olga V. Przhonska,^{†,‡} Artem E. Masunov,^{§,||,¶,∞,Δ} Andriy O. Gerasov,[⊥] Alexey D. Kachkovski,[⊥] Yurii L. Slominsky,[⊥] Alexey I. Tolmachev,[⊥] Vladimir V. Kurdyukov,[⊥] Olexander O. Viniychuk,[⊥] Emma Barrasso,[#] Richard Lepkowicz,[#] David J. Hagan,[†] and Eric W. Van Stryland[†]

[†]CREOL, The College of Optics and Photonics, University of Central Florida, Orlando, Florida 32816, [‡]Institute of Physics, National Academy of Sciences, Kiev 03028, Ukraine, [§]NanoScience Technology Center, University of Central Florida, Orlando, Florida 32826, ^{||}NanoScience Technology Center, University of Central Florida, Orlando, Florida 32826, [¶]Department of Chemistry, University of Central Florida, Orlando, Florida 32816, [∞]Department of Physics, University of Central Florida, Orlando, Florida 32816, ^ΔFlorida Solar Energy Center, University of Central Florida, Cocoa, Florida 32922, [⊥]Institute of Organic Chemistry, National Academy of Sciences, Kiev 03094, Ukraine, and [#]Physics and Optical Engineering, Rose-Hulman Institute of Technology, Terre Haute, Indiana 47803

ABSTRACT The photophysical properties of two pairs of squaraine molecules where two oxygen atoms in a squaraine bridge are replaced with sulfur atoms are investigated. This substitution leads to an inversion of the lowest singlet $\pi-\pi^*$ electronic transition by an $n-\pi^*$ transition, effectively reducing the energy difference between singlet and triplet states and significantly increasing the intersystem crossing efficiency without the use of “heavy atoms”. Experimental results, in agreement with quantum chemical calculations, show near-unity values for triplet quantum yield and singlet oxygen generation quantum yield for sulfur-containing squaraines, which are potentially useful for two-photon photodynamic therapy.

SECTION Molecular Structure, Quantum Chemistry, General Theory



Molecular-based optical materials that exhibit strong excited-state absorption (ESA), both singlet–singlet (S–S) and triplet–triplet (T–T), are of great interest in research areas concerning all optical power control for applications involving lasers with different pulse widths from femto- to nanoseconds.¹ Designing molecules that have both large S–S and T–T ESA processes is challenging. Typically, organic molecules exhibiting strong S–S ESA are characterized by relatively small intersystem crossing rates, limiting the population of their triplet excited states and thus decreasing the intensity of the T–T absorption. Another important application for molecules with large intersystem crossing rates pertains to the generation of singlet molecular oxygen $O_2(a^1\Delta_g)$, which is known to be involved in many photochemical and photobiological processes, specifically concerning sensitizers for photodynamic therapy (PDT).^{2–4} PDT treatment combines drug delivery by a molecular sensitizer upon illumination of an appropriate wavelength (typical within the therapeutic window of 600–1000 nm, where scattered light is minimized and the penetration depth is maximized) to create $O_2(a^1\Delta_g)$, which destroys abnormal cells.⁵ Over the past decades, the generation of $O_2(a^1\Delta_g)$ under one-photon excitation of a molecular sensitizer has been extensively studied.^{5–7} Recent interest in PDT has shifted toward development of two-photon-absorbing (2PA) sensitizers

due to the possibility of applying the advantages of two-photon excitation in the field of medicine and microbiology.^{2,5,8,9}

In this Letter, we discuss the design of photosensitizing molecules with both large triplet quantum yields (Φ_T) and quantum yields of singlet oxygen generation (Φ_Δ), as well as large 2PA cross sections (δ_{2PA}). For many years, our research group has developed new molecules and investigated structure–property relations in order to find larger optical nonlinearities required for various applications. Linear π -conjugated polymethine-like molecules exhibit large δ_{2PA} (up to 30 000 GM)¹⁰ and S–S ESA cross sections (up to 10^{-15} cm²)¹¹ but typically do not possess significant Φ_T .^{4,7,8} A common strategy for enhancing triplet yields is to enhance spin–orbit coupling by the introduction of atoms of large atomic number into either the molecular structure or the host solvent, leading to an increase in the probability of intersystem crossing (the “heavy atom” effect).¹² However, this strategy has been mostly unsuccessful in polymethine molecules.

In this work, we study cationic polymethine dyes (PD), traditional oxygen-containing squaraines (SD–O), and new

Received Date: March 23, 2010

Accepted Date: July 6, 2010

Published on Web Date: July 14, 2010

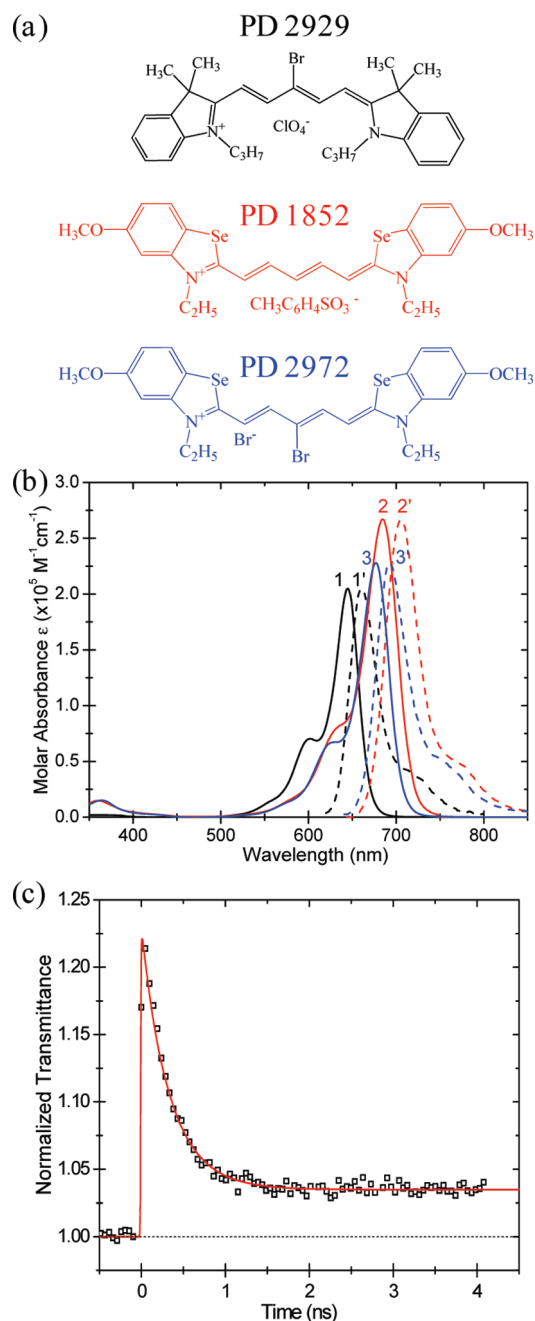


Figure 1. (a) Molecular structures of PD 2929, PD 1852, and PD 2972. (b) Molar absorbance (1, 2, 3) and the normalized fluorescence (1', 2', 3') for PD 2929 (1, 1'), PD 1852 (2, 2'), and PD 2972 (3, 3') in ethanol. (c) Example of decay kinetics for PD 2929 in ethanol with pump and probe at 640 nm.

sulfur-containing squaraines (SD-S). Squaraines can also be considered as compounds from the polymethine family as they combine the polymethine (odd) type of conjugated chain with the squaraine acceptor fragment in D- π -A- π -D structures. Recent work by Salice et al.⁷ has shown a particular group of SD-O to be poor singlet oxygen sensitizers, but they function better as singlet oxygen quenchers. This is due to intramolecular charge transfer (CT) in the squaraines and intramolecular CT of

Table 1. Photophysical parameters^a

	$\lambda_{\text{Abs}}^{\text{max}}$ (nm)	ϵ^{max} ($\times 10^5 \text{ M}^{-1} \text{ cm}^{-1}$)	$\lambda_{\text{Fluor}}^{\text{max}}$ (nm)	Φ_{F}	τ_{F} (ns)	σ_{S1in} ($\times 10^{-16} \text{ cm}^{-2}$)	σ_{T1in} ($\times 10^{-16} \text{ cm}^{-2}$)	τ_{ISC} (ns)	Φ_{T}	Φ_{Δ}	τ_{Triplet} (ns)
PD 2929 EtOH	645	2.67	660	0.10 \pm 0.01	0.28 \pm 0.04	9.5 (640 nm)	7.4 \pm 0.7 (640 nm)	6 \pm 1	0.05 \pm 0.02		
PD 1852 EtOH	685	2.05	706	0.53 \pm 0.03	1.26 \pm 0.19	7.7 (680 nm)	0	6.7 \pm 0.5	0.15 \pm 0.05		290 \pm 30
PD 2972 EtOH	677	2.28	692	0.16 \pm 0.02	0.55 \pm 0.08	7.8 (670 nm)	7.0 \pm 0.7 (670 nm)	5.7 \pm 0.5	0.07 \pm 0.02		70 \pm 10
SD-O 2405 TOL [ACN]	636 [641]	3.65 [3.32]	646 [659]	0.95 \pm 0.05 [0.18 \pm 0.02]	2.3 \pm 0.3 [0.47 \pm 0.07]	5.4 $\times 10^{-2}$ (500 nm)	4.2 \pm 0.6 (500 nm)		< 0.01		
SD-S 7508 TOL	687	1.57	NA	< 0.001	NA	0.57 (460 nm)	4.5 \pm 0.6 (460 nm)		0.97 \pm 0.07	1.0 \pm 0.2	245 \pm 20
SD-O 7560 ACN	351	0.44	NA	< 0.001	NA						
SD-S 7543 ACN	427	0.39	NA	< 0.001	NA	1.4 (430 nm)	0.45 \pm 0.06 (430 nm)	{8.5 \pm 0.2} $\times 10^{-3}$	0.94 \pm 0.03	0.65 \pm 0.13	180 \pm 20

^a $\lambda_{\text{Abs}}^{\text{max}}$ and ϵ^{max} are the peak absorption wavelength and peak extinction coefficient for the lowest-energy transition, $S_0 \rightarrow S_1$; $\lambda_{\text{Fluor}}^{\text{max}}$ is the peak fluorescence wavelength; Φ_{F} and τ_{F} are the measured fluorescence quantum yield and the calculated fluorescence lifetime using ref 15; σ_{S1in} , σ_{T1in} , and σ_{T1in} are ground-state, singlet-singlet and triplet-triplet excited-state cross sections at the indicated wavelengths, respectively; τ_{F} Measured is the measured singlet decay lifetime; τ_{ISC} , Φ_{T} , Φ_{Δ} , and τ_{Triplet} are the intersystem crossing time, triplet yield, quantum yields of singlet oxygen generation, and measured triplet lifetimes, respectively. Note the use of solvent abbreviations: ethanol (EtOH), toluene (TOL), and acetonitrile (ACN).

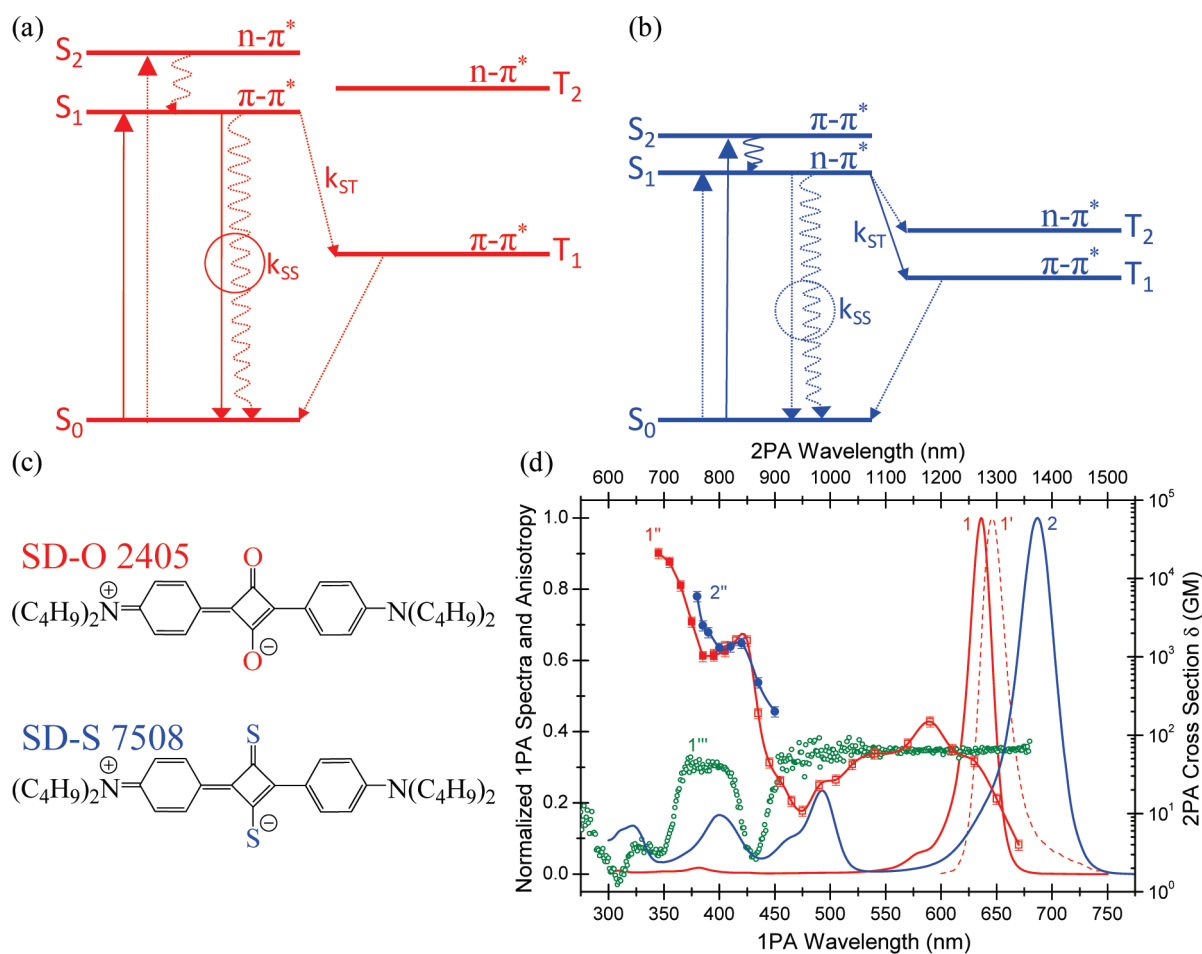


Figure 2. Schematic of energy level structures and the nature of transitions for (a) SD-O and (b) SD-S. Solid line transitions are more probable than dotted line transitions. (c) Molecular structures of SD-O 2405 and SD-S 7508. (d) Normalized one-photon absorption (1, 2), fluorescence (1'), excitation anisotropy in *p*-THF (1'''), and two-photon absorption spectra (1'', 2'') for SD-O 2405 (1, 1', 1'', 1''') and SD-S 7508 (2, 2''). The two-photon excitation wavelengths and absorption cross sections are shown on the right and top axes. 2PA data are obtained by both 2PF (red open squares for SD-O 2405) and open-aperture Z-scan (solid red squares for SD-O 2405 and solid blue circles for SD-S 7508). All spectra are in toluene, except where otherwise noted.

the squaraine–oxygen complex, limiting their triplet yield to less than 15%. In the current work, the triplet yields of our SD-O molecules are believed to be limited by similar CT processes. However, the SD-S structures exhibit a lowering of the energy of the $n-\pi^*$ singlet state, so that it becomes the lowest excited singlet. The lifetime of this “dark state” is long enough for efficient intersystem crossing into the nearby in energy $\pi-\pi^*$ triplet state, producing near-unity triplet quantum yields.

Figure 1 shows molecular structures of three cationic polymethine dyes; the first contains a Br atom substitution within the π -conjugated chain (labeled PD 2929), the second contains Se atoms incorporated into the terminal groups (labeled PD 1852), and the third contains both Se-substituted terminal groups and a Br atom substitution within the π -conjugated chain (labeled PD 2972). The details on compound synthesis and characterization can be found in the Supporting Information, and their main spectroscopic parameters are shown in Table 1.

Our experimental studies (see Experimental Section for details) show that Φ_T for all of the structures shown in

Figure 1a do not exceed 0.15 ± 0.05 , indicating that the internal conversion via singlet states is a dominant deactivation pathway. The use of iodobenzene solvent (heavy atom solvent) instead of ethanol does not significantly increase Φ_T . These results have been explained by our quantum chemical calculations at the TD-B3LYP/6-31G*/PCM level, showing that Br and Se atom substitutions do not affect the charge distribution within the frontier orbitals, HOMO and LUMO, which are responsible for the main $S_0 \rightarrow S_1$ transition for these molecular structures. Thus, these molecular arrangements (containing heavy atoms) are not sufficient to significantly influence the spin–orbit coupling probability, contrary to the common belief.

We propose a different approach to achieve an efficient intersystem crossing process in polymethine-like dyes by engineering the molecular energy level structures in such a way that the singlet–triplet energy difference (or splitting energy) is significantly reduced. Shown in Figure 2a,b are schematics of the nature of the energy level structures of the lowest transitions for SD-O (a) and SD-S (b) molecules. This approach is based on mixing of the spin multiplicities by

inserting lower-lying $n-\pi^*$ transitions involving the unshared pair of electrons. The effect of oxygen and sulfur atoms on the intersystem crossing rate in squaraine molecules is determined by their unshared electron pair. It is known that in molecules whose lowest singlet state is of $\pi-\pi^*$ nature (as for SD-O) the spin-coupling probability is vanishingly small due to a large splitting energy.¹⁵ However, an inversion of the lowest $\pi-\pi^*$ transition by an $n-\pi^*$ transition (as for SD-S) can lead to an enhancement of intersystem crossing efficiency from the singlet state of $n-\pi^*$ to the triplet state of $\pi-\pi^*$ (El-Sayed rule).¹⁴ In this work, we experimentally and theoretically investigate two pairs of SD-S and SD-O molecules, whose structures are shown in Figure 2c and Figure 4a. As predicted by quantum chemical calculations, the sulfur atom substitution leads to the appearance of a lower-lying $n-\pi^*$ singlet state that efficiently overlaps with the strong $\pi-\pi^*$ transition, thus increasing the intersystem crossing rate without the use of heavy atoms.

The absorption spectrum of SD-O 2405 exhibits a strong $S_0 \rightarrow S_1$ $\pi-\pi^*$ transition with a peak molar absorbance of $364\,000\text{ M}^{-1}\text{ cm}^{-1}$ (toluene) and low-intensity $S_0 \rightarrow S_n$ transitions into higher-lying electronic states. Excitation anisotropy valleys indicate large angles between the absorption $S_0 \rightarrow S_n$ and emission $S_1 \rightarrow S_0$ transition dipole moments, indicating the positions of one-photon forbidden transitions, which are allowed in 2PA due to symmetry rules. The fluorescence quantum yield of SD-O 2405 in toluene is large, $\Phi_F = 0.95 \pm 0.05$, which corresponds to a lifetime of 2.3 ns (calculated using the Strickler–Berg equation¹⁵ and measured experimentally¹⁶). Φ_F of SD-O 2405 in polar ACN is much smaller, $\Phi_F = 0.18 \pm 0.02$ (lifetime is 0.5 ns), which, as indicated in ref 7, may be connected with the formation of a lower-energy dark state having charge-transfer character. Removal of oxygen from the ACN solution does not affect the Φ_F value. SD-S 7508 has a comparatively broader, red-shifted ($\sim 50\text{ nm}$) linear absorption band with a peak molar absorbance of $157\,000\text{ M}^{-1}\text{ cm}^{-1}$ (toluene) and several intense $S_0 \rightarrow S_n$ transitions into higher-lying electronic levels. No fluorescence is observed ($\Phi_F < 0.001$), which is explained by the fast intersystem crossing process within $\sim 7\text{ ps}$. Extremely large, near-unity values of Φ_T and Φ_Δ have been determined for SD-S 7508, which, to the best of our knowledge, are the largest currently reported values for PD-like molecules ($\Phi_\Delta = 0.68$ was stated for amino-SD with benzo-selenazole terminal groups due to their heavy atom effect).¹⁷ All primary spectroscopic parameters are shown in Table 1.

2PA spectra are shown in Figure 2d for both SD-O 2405 and SD-S 7508. SD-O 2405 exhibits three 2PA bands. The first 2PA band (vibronic coupling band) with $\delta_{2PA}^{\text{max}} = 200\text{ GM}$ occurs at an energy blue shifted by $\sim 1000\text{--}1200\text{ cm}^{-1}$ as compared to the peak of the $S_0 \rightarrow S_1$ transition. The positions of the second 2PA band with $\delta_{2PA}^{\text{max}} = 2000\text{ GM}$ (at 850 nm) and the third strongest 2PA band with $\delta_{2PA}^{\text{max}} = 15\,000\text{ GM}$ (at 700 nm) correspond to the S_2 and S_4 final states, as indicated by anisotropy and supported by quantum chemical calculations. The 2PA spectrum of SD-S 7508 is similar to the shape for SD-O 2405 in the range of the second 2PA band; however, the high-energy peak cannot be reached due to the $\sim 50\text{ nm}$ red shift and slight broadening of the linear absorp-

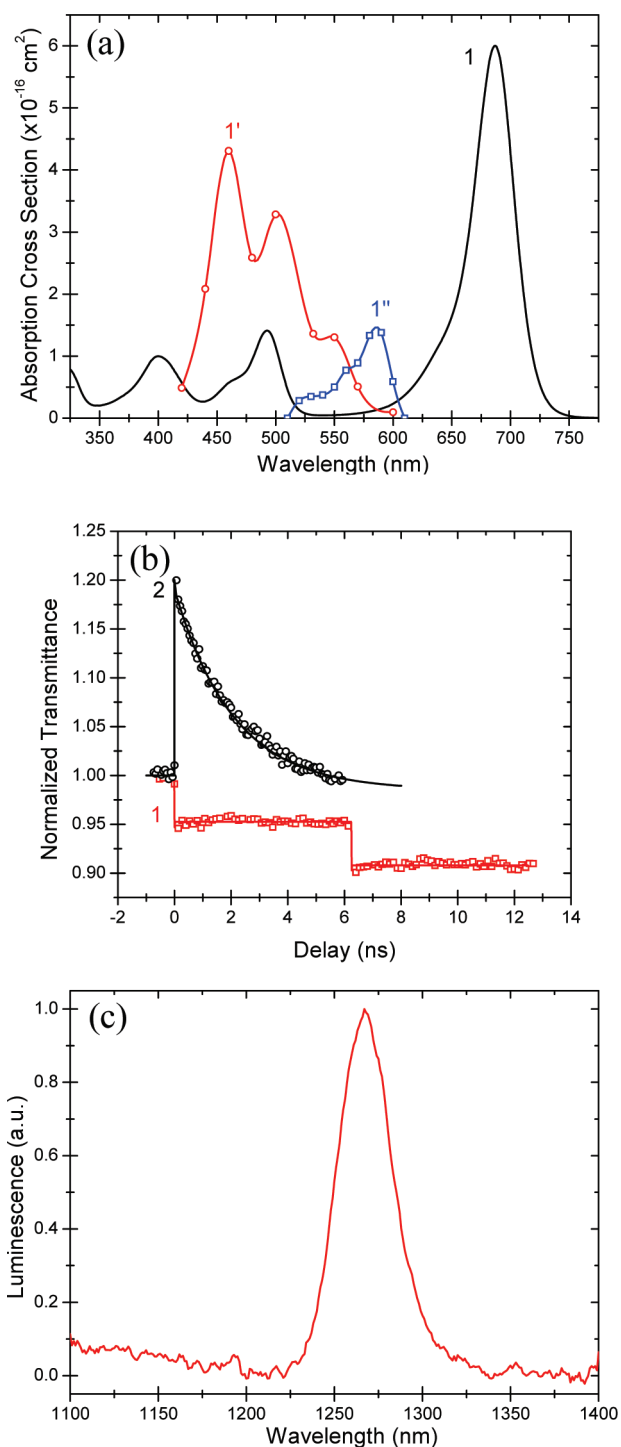


Figure 3. (a) Linear (1), singlet–singlet (1'), and triplet–triplet (1'') excited-state absorption spectra for SD-S 7508 in toluene. (b) Decay kinetics for SD-S 7508 with pump and probe at 550 nm (1) and SD-O 2405 at 650 nm (2) in toluene. (c) Singlet oxygen luminescence spectrum for SD-S 7508 at 680 nm pump in ACN.

tion band. The largest $\delta_{2PA} = 7000\text{ GM}$ for SD-S 7508 was observed at 760 nm. $\text{O}_2(a^1\Delta_g)$ generation was observed via two-photon excitation at 760 nm and confirmed by the quadratic dependence of the singlet oxygen luminescence

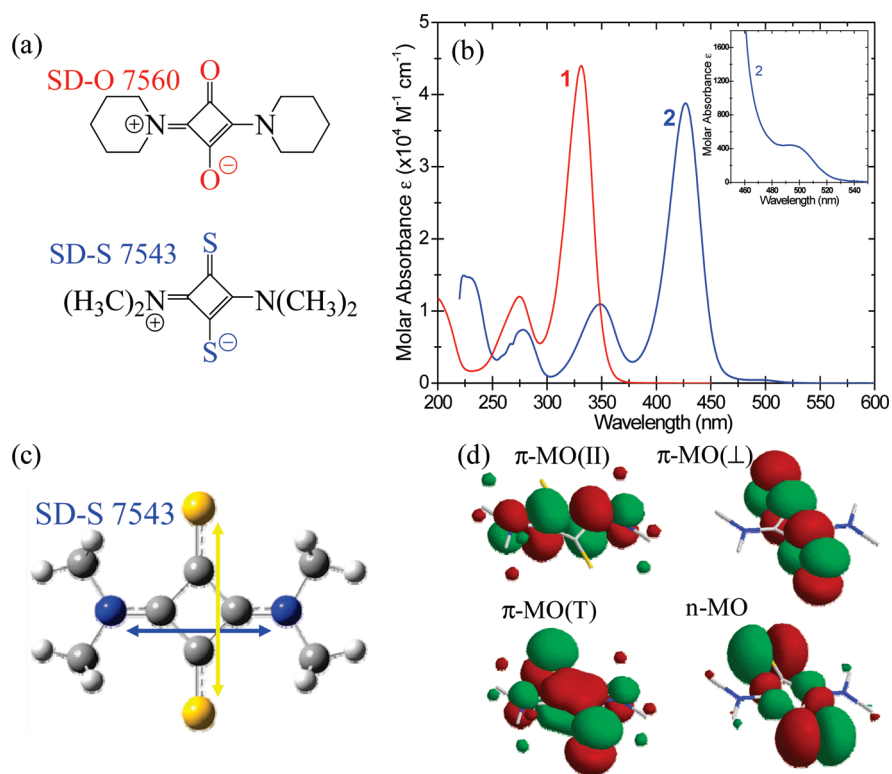


Figure 4. (a) Molecular structures of SD-O 7560 and SD-S 7543. (b) Molar absorbance spectra for SD-O 7560 (1) and SD-S 7543 (2) in ACN. The inset shows the long wavelength absorption tail of SD-S 7543. (c) Molecular schematic for SD-S 7543 showing two perpendicular chromophores, one between nitrogen (dark blue) atoms and the second between sulfur (yellow) atoms. (d) Different types of molecular orbitals for SD-S 7543 (see the description in the text).

at 1270 nm with excitation power (data shown in Figure S1, Supporting Information). The merit parameter for PDT, which describes the molecular ability to generate $\text{O}_2(\text{a}^1\Delta_g)$, is the product of the 2PA cross section and quantum yield of $\text{O}_2(\text{a}^1\Delta_g)$ generation, $\delta_{2\text{PA}} \times \Phi_{\Delta}$. For SD-S 7508, this merit parameter is 7000 at 780 nm, which is comparable to the largest reported values, which occur in porphyrin dimers.¹⁸

In order to better understand intramolecular dynamics in SD-O and SD-S, we apply femto-, pico-, and nanosecond pump-probe techniques to measure the time evolution of the S-S and T-T absorption and their cross sections (σ_{SS} and σ_{TT}). S-S and T-T ESA spectra for SD-S 7508 are shown in Figure 3a. SD-O 2405 possesses one S-S ESA band with a spectral peak at 500 nm ($\sigma_{\text{SS}} = 4.2 \times 10^{-16} \text{ cm}^{-1}$) and shows a nearly complete ground-state recovery (both in toluene and ACN) within 6 ns, shown in Figure 3b, indicating negligible $\Phi_{\text{T}} \leq 0.01$, which is explained by a higher-lying $n-\pi^*$ transition (connected with the unshared pair of electrons of the oxygen atoms) as compared to SD-S 7508. The S-S ESA absorption for SD-S 7508, with spectral peaks at 460 ($\sigma_{\text{SS}} = 4.3 \times 10^{-16} \text{ cm}^{-1}$) and 500 nm ($\sigma_{\text{SS}} = 3.3 \times 10^{-16} \text{ cm}^{-1}$), decays with a lifetime of ~ 4.5 ps, while a long-lived T-T absorption at 590 nm ($\sigma_{\text{TT}} = 1.4 \times 10^{-16} \text{ cm}^{-1}$) is populated on a similar time scale. The triplet quantum yield and T-T cross section are determined from the double pump-probe technique (see Experimental Section) to be $\Phi_{\text{T}} \approx 0.9 \pm 0.1$ (Figure 3b). The triplet state lifetime for SD-S 7508 in air-saturated toluene solution is 250 ns (results for the other molecules are listed in Table 1).

We also investigated two squaraine dyes, SD-S 7543 and SD-O 7560, which absorb in the UV-vis spectral region with molecular structures shown in Figure 4a. These dyes do not fluoresce ($\Phi_{\text{F}} < 0.001$), however, for different reasons. SD-O 7560 shows a complete ground-state recovery in ~ 7 ps, signifying negligible Φ_{T} with the main decay channel via internal conversion processes. SD-S 7543 exhibits a similar decay time, resulting in the population of the triplet state with large $\Phi_{\text{T}} \approx 0.94 \pm 0.03$ and $\Phi_{\Delta} = 0.65 \pm 0.13$. Quantum chemical calculations at the TD-B3LYP/6-31G*/PCM level allow the determination of the energy positions and the nature of the lowest electronic singlet and triplet transitions.

Calculations show that a squaraine molecule consists of two perpendicular π -conjugated chromophores; one is placed in the horizontal plane between the two nitrogen atoms, and the second is placed in the vertical plane between two sulfur (or oxygen) atoms, as shown in Figure 4c for SD-S 7543. Four types of molecular orbitals (MO) are responsible for the lowest electronic transitions and are shown for SD-S 7543 in Figure 4d. HOMO represents the orbital totally delocalized within the whole molecule (T); HOMO-1 is the n-MO involving the unshared pair of electrons of sulfur atoms; LUMO and LUMO+1 are two π -MOs involving charge distributed only within the vertical (\perp) or horizontal (\parallel) chromophores. The lowest electronic transition, HOMO-1 \rightarrow LUMO, is of the $n-\pi^*$ nature and can be seen in Figure 4b as a small band at ~ 500 nm. The next HOMO \rightarrow LUMO transition is of the $\pi-\pi^*$ nature and represents an intense band with a peak position at 427 nm. Calculations

suggest that replacing the oxygen atoms with sulfur results in an inversion of the lowest $\pi-\pi^*$ transition by an $n-\pi^*$ transition, effectively mixing the singlet and triplet states of different nature, thus enhancing the intersystem crossing efficiency.

In summary, we propose a new approach of developing polymethine-like molecules having large triplet and singlet oxygen generation quantum yields (up to 100%), large two-photon absorption cross sections (up to 7000 GM within the therapeutic window), and large S-S and T-T absorption cross sections (up to $4 \times 10^{-16} \text{ cm}^2$), potentially useful as efficient sensitizers for PDT and optical power regulation applications.

EXPERIMENTAL SECTION

Linear absorption spectra and fluorescence spectra were recorded by a Varian Cary 500 spectrophotometer and a PTI QuantaMaster spectrofluorometer, respectively. Fluorescence quantum yields were determined with excitation within the main absorption band at peak optical densities not exceeding 0.1 (10 mm cell) by the standard method relative to cresyl violet perchlorate in methanol. The direct measurements of singlet oxygen luminescence at $\sim 1270 \text{ nm}$ were performed in air-saturated ACN at room temperature using a PTI QuantaMaster spectrofluorometer with a nitrogen-cooled Hamamatsu R5509-73 photomultiplier tube detector at the steady-state regime. $\text{O}_2(a^1\Delta_g)$ generation quantum yields were measured in comparison with acridine in ACN with $\Phi_{\Delta} = 0.82$.¹⁹ Fluorescence lifetimes were obtained by polarization-resolved pico- and femtosecond pump-probe techniques.¹⁶ 2PA spectra were measured with femtosecond pulses by the 2PF²⁰ and Z-scan²¹ techniques for SD-O 2405 and nonfluorescent SD-S 7508. 2PA and femtosecond pump-probe measurements were performed using two optical parametric generator/amplifiers (model TOPAS-800 pumped by a Clark-MXR CPA-2010 at a 1 kHz repetition rate), which can be tuned independently with pulsewidths of $\sim 135 \text{ fs}$ (fwhm). The femtosecond pump-probe technique was used to verify the instantaneous 2PA response and the absence of ESA contribution to $\delta_{2\text{PA}}$ values.²² The S-S and T-T ESA spectra were measured using the femtosecond pump and white-light continuum probe technique.²³ To determine σ_{SS} and σ_{TT} , femto- and picosecond Z-scan measurements were used and modeled with a five-level system including singlet and triplet excited states. In order to independently determine Φ_{T} and σ_{TT} , we utilized picosecond double pump-probe²⁴ and singlet depletion²⁵ techniques.

SUPPORTING INFORMATION AVAILABLE Chemical synthesis and characterization and singlet oxygen luminescence via two-photon absorption. This material is available free of charge via the Internet at <http://pubs.acs.org>.

AUTHOR INFORMATION

Corresponding Author:

*To whom correspondence should be addressed. E-mail: swebster@creol.ucf.edu.

ACKNOWLEDGMENT We gratefully acknowledge support of the U.S. Army Research Laboratory W911NF0420012, the U.S. Army Research Laboratory, and the U.S. Army Research Office under

Contract/Grant number 50372-CH-MUR, the NSF/CRC program CHE0832622, and the Office of Naval Research MORPH N00014-06-1-0897.

REFERENCES

- (1) Tutt, L. W.; Boggess, T. F. A Review of Optical Limiting Mechanisms and Devices Using Organics, Fullerenes, Semiconductors and Other Materials. *Prog. Quantum Electron.* **1993**, *17*, 299–338.
- (2) Beverina, L.; Crippa, M.; Landenn, M.; Ruffo, R.; Salice, P.; Silvestri, F.; Versari, S.; Villa, A.; Ciaffoni, L.; Collini, E.; Ferrante, C.; Bradamante, S.; Mari, C. M.; Bozio, R.; Pagani, G. A. Assessment of Water-Soluble π -Extended Squaraines as One- and Two-Photon Singlet Oxygen Photosensitizers: Design, Synthesis, and Characterization. *J. Am. Chem. Soc.* **2008**, *130*, 1894–1902.
- (3) Ramaiah, D.; Joy, A.; Chandrasekhar, N.; Eldho, N. V.; Das, S.; George, M. V. Halogenated Squaraine Dyes as Potential Phototherapeutic Agents. Synthesis and Study of Photophysical Properties and Quantum Efficiencies of Singlet Oxygen Generation. *Photochem. Photobiol.* **1997**, *65*, 783–790.
- (4) Santos, P. F.; Reis, L. V.; Duarte, I.; Serrano, J. P.; Almeida, P.; Oliveira, A. S.; Vieira Ferreira, L. F. Synthesis and Photochemical Evaluation of Iodinated Squarylium Cyanine Dyes. *Helv. Chim. Acta* **2005**, *88*, 1135–1145.
- (5) Schweitzer, C.; Schmidt, R. Physical Mechanisms of Generation and Deactivation of Singlet Oxygen. *Chem. Rev.* **2003**, *103*, 1685–1757.
- (6) DeRosa, M. C.; Crutchley, R. J. Photosensitized Singlet Oxygen and its Applications. *Coord. Chem. Rev.* **2002**, *233/234*, 351–371.
- (7) Salice, P.; Arnbjerg, J.; Pedersen, B. W.; Toftgaard, R.; Beverina, L.; Pagani, G. A.; Ogilby, P. R. Photophysics of Squaraine Dyes: Role of Charge-Transfer in Singlet Oxygen Production and Removal. *J. Phys. Chem. A* **2010**, *114*, 2518–2525.
- (8) Ogawa, K.; Kobuke, Y. Recent Advances in Two-Photon Photodynamic Therapy. *Anticancer Agents Med. Chem.* **2008**, *8*, 269–279.
- (9) Nielsen, C. B.; Arnbjerg, J.; Johnsen, M.; Jrgensen, M.; Ogilby, P. R. Molecular Tuning of Phenylene-Vinylene Derivatives for Two-Photon Photosensitized Singlet Oxygen Production. *J. Org. Chem.* **2009**, *74*, 9094–9104.
- (10) Chung, S. J.; Zheng, S.; Odani, T.; Beverina, L.; Fu, J.; Padilha, L. A.; Biesso, A.; Hales, J. M.; Zhan, X.; Schmidt, K.; et al. Extended Squaraine Dyes with Large Two-Photon Absorption Cross-Sections. *J. Am. Chem. Soc.* **2006**, *128*, 14444–14445.
- (11) Padilha, L. A.; Webster, S.; Hu, H.; Przhonska, O. V.; Hagan, D. J.; Van Stryland, E. W.; Bondar, M. V.; Davydenko, I. G.; Slominsky, Y. L.; Kachkovski, A. D. Excited State Absorption and Decay Kinetics of Near IR Polymethine Dyes. *Chem. Phys.* **2008**, *352*, 97–105.
- (12) Lower, S. K.; El-Sayed, M. A. The Triplet State and Molecular Electronic Processes in Organic Molecules. *Chem. Rev.* **1966**, *66*, 199–241.
- (13) Dewar, M. J. S. *The Molecular Orbital Theory of Organic Chemistry*; McGraw-Hill: New York, 1969.
- (14) El-Sayed, M. A. Spin-Orbit Coupling and the Radiationless Processes in Nitrogen Heterocyclics. *J. Chem. Phys.* **1963**, *38*, 2834–2837.
- (15) Strickler, S. J.; Berg, R. A. Relationship Between Absorption Intensity and Fluorescence Lifetime of Molecules. *J. Chem. Phys.* **1962**, *37*, 814–822.
- (16) Przhonska, O. V.; Hagan, D. J.; Novikov, E.; Lepkovicz, R.; Van Stryland, E. W.; Bondar, M. V.; Slominsky, Y. L.; Kachkovski,

- A. D. Picosecond Absorption Anisotropy of Polymethine and Squarylium Dyes in Liquid and Polymeric Media. *Chem. Phys.* **2001**, *273*, 235–248.
- (17) Santos, P. F.; Reis, L. V.; Almeida, P.; Oliviera, A. S.; Viera Ferriera, L. F. Singlet Oxygen Generation Ability of Squarylium Cyanine Dyes. *J. Photochem. Photobiol., A* **2003**, *160*, 159–161.
- (18) Drobizhev, M.; Stepanenko, Yu.; Dzenis, Yu.; Karotki, A.; Rebane, A.; Taylor, P.; Anderson, H. Extremely Strong Near-IR Two-Photon Absorption in Conjugated Porphyrin Dimers. *J. Phys. Chem. B* **2005**, *109*, 7225–7236.
- (19) Wilkinson, F.; P. Helman, W.; Ross, A. B. Quantum Yields for the Photosensitized Formation of the Lowest Electronically Excited Singlet State of Molecular Oxygen in Solution. *J. Phys. Chem. Ref. Data* **1993**, *22*, 113–262.
- (20) Xu, C.; Webb, W. W. Measurement of Two-Photon Excitation Cross Sections of Molecular Fluorophores with Data from 690 to 1050 nm. *J. Opt. Soc. Am. B* **1996**, *13*, 481–491.
- (21) Sheik Bahae, M.; Said, A. A.; Van Stryland, E. W. High-Sensitivity, Single-Beam n² Measurements. *Opt. Lett.* **1989**, *14*, 955–957.
- (22) Webster, S.; Fu, J.; Padilha, L. A.; Przhonska, O. V.; Hagan, D. J.; Van Stryland, E. W.; Bondar, M. V.; Slominsky, Y. L.; Kachkovski, A. D. Comparison of Nonlinear Absorption in Three Similar Dyes: Polymethine, Squaraine and Tetraone. *Chem. Phys.* **2008**, *348*, 143–151.
- (23) Negres, R. A.; Przhonska, O. V.; Hagan, D. J.; Van Stryland, E. W.; Bondar, M. V.; Slominsky, Y. L.; Kachkovski, A. D. The Nature of Excited-State Absorption in Polymethine and Squarylium Molecules. *IEEE J. Select. Top. Quantum Electron.* **2001**, *7*, 849–863.
- (24) Swatton, S. N.; Welford, K. R.; Hollins, R. C.; Sambles, J. R. A Time Resolved Double Pump–Probe Experimental Technique to Characterize Excited-State Parameters of Organic Dyes. *Appl. Phys. Lett.* **1997**, *71*, 10–12.
- (25) Lessing, H. F.; Von Jena, A.; Reichert, M. Triplet Yield Determination and Heavy-Atom Effect from Ground-State Repopulation Kinetics. *Chem. Phys. Lett.* **1976**, *42*, 218–222.